J. Hydrol. Hydromech., 63, 2015, 2, 110–116
DOI: 10.1515/johh-2015-0023

New automatic minidisk infiltrometer: design and testing

Vladimír Klípa, Michal Sněhota*, Michal Dohnal

Czech Technical University in Prague, Faculty of Civil Engineering, Thákurova 7, 166 29 Prague 6, Czech Republic.
*Corresponding author. Tel.: +420 224354748. Fax: +420 233337005. E-mail: michal.snehota@fsv.cvut.cz

Abstract: Soil hydraulic conductivity is a key parameter to predict water flow through the soil profile. We have developed an automatic minidisk infiltrometer (AMI) to enable easy measurement of unsaturated hydraulic conductivity using the tension infiltrometer method in the field. AMI senses the cumulative infiltration by recording change in buoyancy force acting on a vertical solid bar fixed in the reservoir tube of the infiltrometer. Performance of the instrument was tested in the laboratory and in two contrasting catchments at three sites with different land use. Hydraulic conductivities determined using AMI were compared with earlier manually taken readings. The results of laboratory testing demonstrated high accuracy and robustness of the AMI measurement. Field testing of AMI proved the suitability of the instrument for use in the determination of sorptivity and near saturated hydraulic conductivity.

Keywords: Tension infiltrometer; Hydraulic conductivity; Sorptivity; Automated measurement; Infiltration experiment; Zhang's method.

INTRODUCTION

Tension disk infiltrometers are portable inexpensive devices commonly used to determine unsaturated hydraulic conductivity of the soil matrix in the field. The knowledge of the unsaturated hydraulic conductivity is often required to characterize soils with presence of preferential flow (Doležal et al., 2007). Tension infiltration allow determination of a value of soil matrix hydraulic conductivity (Cameira et al., 2003; Vervoort et al., 1999; Vervoort et al., 2003) by elimination of large pores with an air entry value smaller than pressure head set on the infiltrometer. The knowledge both saturated and unsaturated hydraulic conductivities is important for sites where saturated hydraulic conductivity is highly variable due to preferential flow effects attributable to soil structure, significant spatial variability of local soil hydraulic properties and highly conductive pathways along decayed tree roots.

Recently tension disk infiltrometers have been also utilized to investigate the various effects on hydraulic conductivity associated with the filling of macropores (e.g. Holden, 2009; White et al., 1992); temporal changes in soil hydraulic properties caused by tillage practice (e.g. Logsdon and Jaynes, 1996; Schwarzel et al., 2011); effect of crust formation at the soil surface (e.g. Li et al., 2005; Vandervaere et al., 1997); and the effect of water repellency on infiltration (e.g. Lamparter et al., 2006).

Tension infiltrometer typically consists of three parts: porous disk (usually nylon mesh membrane or sintered stainless steel), water reservoir and Mariotte's bottle (suction adjustment). Tension infiltration method is based on application of water at the known constant negative pressure head on the soil surface via porous disk. When disk is in the contact with soil surface, water flows from the water reservoir into the pores. Cumulative infiltration is mostly determined from the drop in water level in the reservoir. Water level in reservoirs of disk infiltrometers is often checked visually by the operator. This method is labour-intensive, especially in soils with low hydraulic conductivity. In order to measure cumulative infiltration data without constant attention of the operator Ankeny et al. (1988) proposed automation of tension infiltration measurement based on use of a pressure sensor that frequently records hydrostatic pressure of the water column in the reservoir tube of the infiltrometer. Madsen and Chandler (2007) proposed the use of a differential pressure sensor for reduction of pressure oscillations related to air-bubble release from the bubbling tube. Gordon and Hallett (2014) suggested a system based on electrical resistivity measurements of the rate of air-bubbles release. This method seems to be suitable for miniature infiltrometers or very low infiltration rates. An alternative approach to automating infiltrometers was proposed by Moret-Fernández et al. (2012). They used a micro-flowmeter to determine the amount of infiltrated water. However the device seems to be overcomplicated and not suitable for use in the field. Moret et al. (2004) suggested water level registration using a time domain reflectometry probe placed in the reservoir tube. Another method proposed by Jara et al. (2012) or Rodný et al. (2013) is based on sequential imaging of water level in the infiltrometer's reservoir using an automatic camera or a smart phone's digital camera. The images thus acquired are subsequently evaluated by particle tracking image analysis.

The aims of this study are threefold: (i) to present a newly developed minidisk infiltrometer capable of automatically reading cumulative infiltration based on buoyancy force acting on a vertical bar immersed in water; (ii) to test the basic functionality of this infiltrometer in the laboratory and (iii) to verify the performance of the infiltrometer under field conditions in three contrasting environments: a crop field and a meadow in an agricultural catchment and a young spruce forest in a mountainous headwater catchment.

MATERIALS AND METHODS

Design of automatic minidisk infiltrometer

The automatic minidisk infiltrometer (AMI) presented in this paper consists of three main parts: the infiltration module, a Mariotte's bottle and a datalogger. The parts of the instrument are detachable in order to ensure portability. Figure 1 is a diagram of the minidisk infiltrometer.

The main part of the minidisk infiltrometer is the infiltration module (see Figure 2). The module utilizes new principle of registering for automated measurements of the infiltration process. The AMI uses a load cell sensor to measure depth of water in the reservoir tube of the infiltration module by sensing the buoyancy force acting on a fixed vertical solid bar.

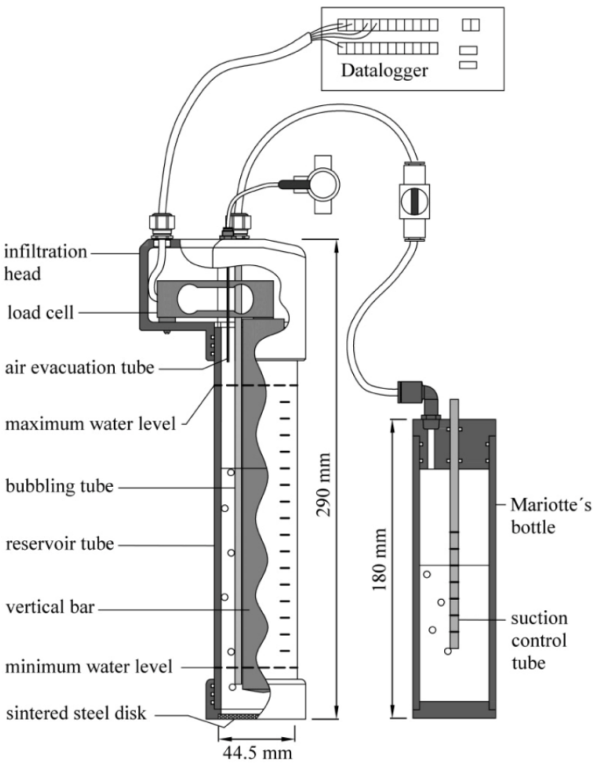

Fig. 1. Scheme of automatic minidisk infiltrometer.

Fig. 2. Infiltration module of the automatic minidisk infiltrometer.

The infiltration module consists of the infiltration head, reservoir tube and an infiltration adapter fitted with the sintered steel disk (44.5 mm diameter). The infiltration head is manufactured from rigid polypropylene using 3D printing technology. The infiltration head together with the infiltration adapter are attached to the upper end of the reservoir tube. The reservoir tube is made of polymethyl methacrylate with internal diameter of 42 mm, and length of 230 mm. The infiltration head covers the bubbling tube, auxiliary air evacuation tube and the load cell sensor. A vertical solid bar (length 225 mm, diameter 25 mm, material: polymethyl methacrylate) is firmly bolted to the load cell. The bottom of the vertical bar is conical, which prevents trapping of bubbles under the bar. The bottom end of the bubbling tube is set 20 mm above the bottom side of the sintered steel disk.

The bubbling tube in the module is connected to the Mariotte's bottle via flexible tubing. Pressure head in the disk can be adjusted in the range: 0.5 to 6 cm. Adjustment of pressure head is accomplished by changing the height of the suction control tube in the Mariotte's bottle.

The infiltration module is refilled by evacuating air from the reservoir via the auxiliary evacuation tube, while the bottom of the infiltration module is placed in a water filled vessel. Removing air from the top of the reservoir causes water to flow through the sintered steel porous disk into the reservoir. The maximum volume of water usable for one infiltration experiment is 190 cm^3.

The load cell (type PW4C3/300G, maximal loading capacity: 300 g, sensitivity 1 ± 0.1 mV/V; Hottinger Baldwin Messtechnik GmbH, Darmstadt, Germany) is connected to a battery powered datalogger (CR1000, Campbell Scientific, Inc., Logan, UT, USA). The datalogger records the changes in the buoyancy force acting on the bar. These changes are directly related to changes in water level. The datalogger analog–digital converter resolution corresponds to 0.01 cm of water level change. According to the load cell manufacturer's specifications, the calculated hysteresis and nonlinearity error is ± 0.018 cm for water level measurement, temperature effect on water level measurement is ± 0.011 cm / 10°C (in the range: + 20°C … + 40°C) and ± 0.007 cm / 10°C (in range: 0°C … + 20°C). Therefore the measurement accuracy of the load cell is consistently better than 0.07% of the rated output.

Principle of operation

Our primary goal is to measure the water level z_i (cm) in the reservoir tube of the infiltration module, where subscript i indicates the i-th measured water level decrease that is detected by the load cell in response to changes in gravity force F_g and buoyancy force F_{bi} acting on the vertical bar

$$F_i = F_g - F_{bi} \tag{1}$$

where F_i is the resultant force acting on the load cell. The load cell then acts in the opposite direction by the reaction force F_{lci} as demonstrated in Figure 3. Rewriting equation 1 using Archimedes' principle yields:

$$F_i = g\left[m_{vb} - \rho_w A_{vb}(z_n - z_i)\right] \tag{2}$$

where g is the gravitational acceleration (m s^{-2}), m_{vb} is vertical bar mass (kg), A_{vb} is cross-sectional area of the vertical bar (m^2), ρ_w is volumetric mass density of water (kg m^{-3}), z_i (m) is the current water level in the storage space of infiltration module and z_n (m) is water level at the level of the end of the solid bar.

In standard operating mode, measurement of water level is taken frequently (every ten seconds) but the new z_i is recorded only when it exceeds the previously recorded z_{i-1} by 0.2 cm. Subsequently, the cumulative infiltration I (cm) and the mean

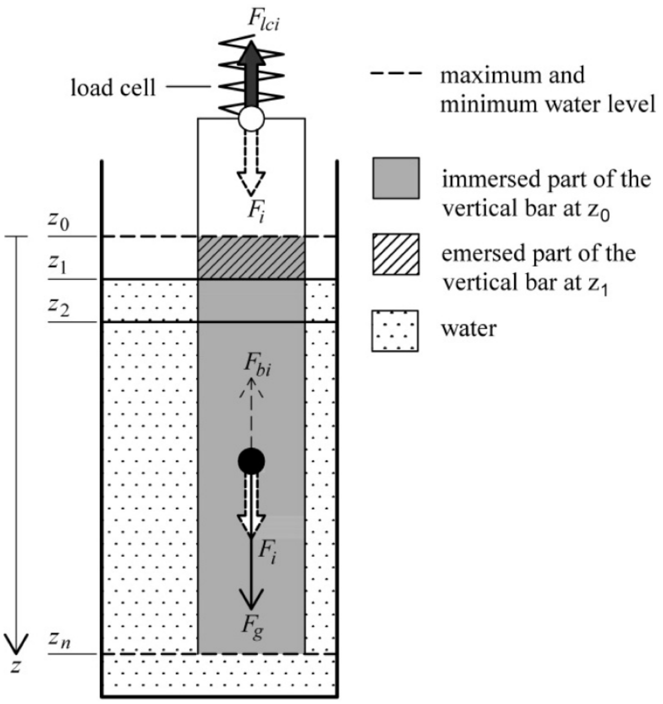

Fig. 3. Principle of water level (z) measurement in the reservoir tube of the infiltration module.

infiltration rate q (cm min^{-1}) are determined for recorded z_i and t_i as follows:

$$I_i = z_i \frac{A_m}{A_s} \tag{3}$$

$$q_i = \frac{(z_i - z_{i-1})A_m}{(t_i - t_{i-1})A_s} \tag{4}$$

where: A_m (m^2) is the cross-sectional area of water in the reservoir tube, and A_s (m^2) is the area of sintered steel disk.

Estimation of sorptivity and hydraulic conductivity

The result of the infiltration experiment using the automatic minidisk infiltrometer is a time sequence of cumulative infiltration values. The first two terms of the Philip approximation are used for a description of the infiltration process below the disk infiltrometer:

$$I = C_1 t^{1/2} + C_2 t \tag{5}$$

where I is the cumulative infiltration (m), t is time (s) and the coefficients C_1 (m s$^{-0.5}$) and C_2 (m s^{-1}) characterize the flow with regard to capillary and gravitational forces under the infiltrometer. Analogously for infiltration rate q (m s^{-1})

$$q = 0.5C_1 t^{-1/2} + C_2 \tag{6}$$

To evaluate the unsaturated hydraulic conductivity and sorptivity the cumulative infiltration data are fitted to equation (5). Zhang (1997) proposed the following relationships for sorptivity S (m s$^{-0.5}$) and unsaturated hydraulic conductivity:

$$C_1 = SA_1 \tag{7}$$

$$C_2 = K_{h0} A_2 \tag{8}$$

where K_{h0} is hydraulic conductivity (m s^{-1}) corresponding to the applied disk pressure head h_0 (m) and the coefficients C_1 and C_2 are determined from the best fit of measured I (t) by function (5). Dimensionless empirical coefficients A_1 and A_2 in the equation (7) and (8) can be calculated for van Genuchten model parameters of the retention curve of a given soil in accordance with Zhang's method modification published by Dohnal et al. (2010):

$$A_1 = \frac{1.4b^{0.5}(\theta_{h0} - \theta_i)^{0.25} \exp\left[3(n-1.9)\alpha h_0\right]}{(\alpha r_0)^{0.15}} \tag{9}$$

$$A_2 = \frac{11.65(n^{0.1} - 1)\exp\left[2.92(n-1.9)\alpha h_0\right]}{(\alpha r_0)^{0.91}} \qquad n \ge 1.9 \tag{10}$$

$$A_2 = \frac{11.65(n^{0.1} - 1)\exp\left[7.5(n-1.9)\alpha h_0\right]}{(\alpha r_0)^{0.91}} \qquad 1.35 \le n < 1.9 \tag{11}$$

$$A_2 = \frac{11.65(n^{0.82} - 1)\exp\left[34.65(n-1.19)\alpha h_0\right]}{(\alpha r_0)^{0.6}} \qquad n < 1.35 \tag{12}$$

where n (–) and α (cm^{-1}) are van Genuchten model parameters of the retention curve and b = 0.55 (Warrick and Broadbridge, 1992), θ_{h0} is the volumetric water content (m^3 m^{-3}) corresponding to the applied pressure head h_0 (m), θ_i is the initial water content (m^3 m^{-3}), r_0 denotes the radius of the infiltration disk (m). The quality of the measured data is usually assessed using differential linearization (see Vandervaere et al., 1997) which can reveal possible loss of hydraulic contact between the soil surface and the sintered steel disk, the effect of the contact sand layer on infiltration (Vandervaere et al., 2000) or significant inhomogeneity of the flow domain.

Laboratory equipment and experimental sites

Laboratory experiments and initial testing of the instrument were performed at the Soil Physics Laboratory (Faculty of Civil Engineering, Czech Technical University in Prague). The following equipment was used: temperature probe 107 (Campbell Scientific, Logan, Utah, USA), peristaltic pump (model Ecoline VC-360 - Ismatec SA, Glattbrugg, CH) and a standard commercially available aerator.

The infiltrometer was further tested at an agricultural catchment and in a mountainous headwater catchment. First one is the Kopaninský Stream experimental catchment (7.1 km^2) that is located in the Vltava River basin, in the Bohemo-Moravian Highland area of the Czech Republic (elevation ranges from 467 to 578 m above sea level, annual precipitation exceeds 665 mm, average annual temperature 7°C). The soil is loamy sand classified as Dystric Cambisol (Tachecí et al., 2013). Two locations selected for testing of AMI in the catchment were a meadow and a cultivated crop field.

The second experimental catchment, Uhlířská, is situated in Jizera Mountains, Czech Republic (total area 1.78 km^2, average altitude 820 m above sea level, annual precipitation exceeding 1300 mm, average annual temperature 4.7°C). Uhlířská is a mountainous catchment undergoing reforestation. The soil at the testing location – a valley hillslope – is shallow sandy loam classified as Dystric Cambisol (Šanda, 1999) The soil has well developed internal structure with a broad range of pore sizes. Automated infiltrometer was in the Uhlířská catchment tested at the hillslope site covered by a young spruce forest.

The retention data for the soils tested were measured in the laboratory on undisturbed 100-cm^3 soil samples by means of the hanging water column desorption method combined with the pressure plate apparatus method (Klute, 1986). The soil hydraulic parameters were derived from the retention data using a van Genuchten approach (van Genuchten, 1980). The soil hydraulic parameters are summarized in Table 1.

Table 1. Hydraulic parameters of the soils used for verification of the instrument.

Parameter/cover		Kopaninský stream meadow	Kopaninský stream crop field	Uhlířská spruce forest
θ_s	(–)	0.530	0.540	0.650
θ_{init}	(–)	0.270	0.280	0.550
α	(cm^{-1})	0.128	0.043	0.026
n	(–)	1.510	1.545	1.163

θ_{init} denotes soil water content before infiltration experiment,
θ_s is saturated water content

RESULTS AND DISCUSSION
Calibration and testing

We performed three types of calibration and testing procedures: short-term pumping test, temperature dependency tests and simple technique to estimate dynamic effects caused by air-bubble release. Two measurement modes were used to produce each measurement point of load cell output. In averaging mode mean value of 20 consecutive readings, taken during approx. 1.2 s, was recorded. In instantaneous mode single reading was taken and no averaging was performed. Short-term pumping test allowed verification of correct sensor function and evaluation of measurement mode (i.e., reading frequency and averaging at logger side). Pumping test was conducted by water removal from the cylinder with immersed vertical bar. Pumping test was performed under constant temperature. Data were recorded in one-minute interval. Infiltration rate induced by the peristaltic pump was 0.3 cm min^{-1}. Good sensor functioning is demonstrated in Fig. 4a and in Fig. 4b for the case of averaged data.

No deviations in measured water level decrease (average mode) were detected in comparison with actual water level decrease (Fig. 4a) calculated from known pumping rate and cross-sectional area of water in the cylinder. Water level decrease measured in instantaneous mode is not shown in Fig. 4a because this data prove nearly the same quality as data measured in average mode. However, sensor measurement mode has a significant impact on results of infiltration rate (Fig. 4b). The calculated infiltration rate is noisy in the instantaneous mode (see Fig. 4b), however the mean infiltration rates are almost identical in both measurement modes (Table 2). Presence of noise in data obtained by instantaneous mode in comparison with data from averaging mode is obvious from Table 2 where standard error of mean, standard deviation and difference between maximum and minimum are several times higher in case of instantaneous mode data than in case of averaged mode data.

Changing temperature during infiltration tests is often responsible for incorrect or inadequate measurement in the field. A six-day test of temperature effects on load cell measurement was performed in the laboratory. Data were recorded in five-second intervals. The vertical bar was left in the air and subjected to six cycles of temperature changes (range 12.75°C). Results in Fig. 5 and Table 3 show the high stability of sensor output during the test. 1-μV change of sensor response corresponds to 0.09 cm change in water level only. Better quality of data measured in averaging mode is obvious. Performed tests document that sensor is relatively insensitive to temperature fluctuations.

Air bubble release from the instrument's bubbling tube could significantly disturb automatic infiltrometer measurement. The effect of pressure oscillations caused by air-bubbles was tested using an aerator generating a strong irregular stream of bubbles. A one-day test with varying infiltration rates was conducted. Data were recorded in five sec. intervals, in averaging mode.

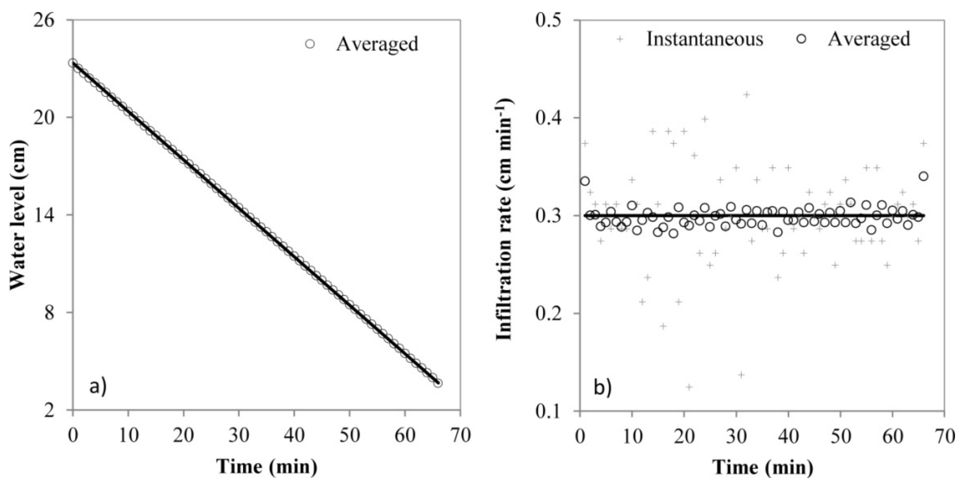

Fig. 4. Sensor readings converted to a) water level and b) infiltration rate in response to constant pumping test. Black lines represent preset pumping rate (right) and corresponding water level decrease (left). Symbols denote one-minute interval reading of the sensor in both instantaneous and average modes.

Table 2. Statistical evaluation of infiltration rate measurement during constant pumping with preset rate 0.3 cm min^{-1}.

	Mean	Std. error of mean	Std. deviation	Minimum	Maximum
Instantaneous data (cm min^{-1})	0.299	0.007	0.055	0.125	0.423
Averaged data (cm min^{-1})	0.298	0.001	0.010	0.281	0.340

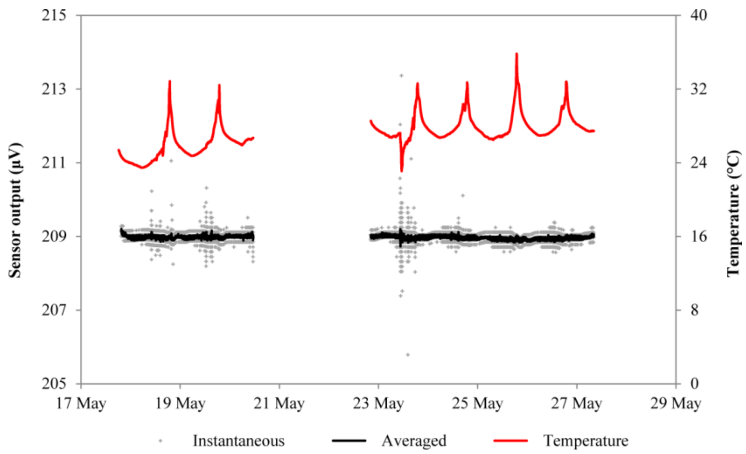

Fig. 5. Sensor performance during six-day test of temperature effects on measurement. Thin black line represents data recorded in average mode and symbols are data recorded in instantaneous mode. Data were recorded in 5-s intervals.

Table 3. Statistical evaluation of temperature dependency test.

	Mean	Std. error of mean	Std. deviation	Minimum	Maximum
Instantaneous data (μV)	208.968	2.4 E–04	0.085	205.7	213.3
Averaged data (μV)	208.969	1.3 E–04	0.045	208.7	209.4
Temperature (°C)	27.090	–	1.880	23.1	35.8

Analysis of three one-hour stages with constant water level shows standard deviations less than 0.015, 0.014 and 0.008 cm. Standard deviation during transient stages never exceeds 0.02 cm. Therefore the operating principle and the sensor used seem to be robust in terms of dynamic effects caused by air-bubble release.

Field application

Automatic minidisk infiltrometer was tested in the Kopaninský Stream experimental catchment on a meadow and on a tilled crop field on August 2th, 2012. The first experiment was conducted on the meadow after the turf was removed, while the second experiment on the tilled crop field was done after post-harvest stubble-breaking. A thin layer (approx. 1 mm) of dry fine quartz sand with grain size ranging between 0.10 and 0.63 mm (ST01/06 PAP, Sklopisek Strelec, Czech Republic) was used to provide the contact between the stainless steel sintered disk of the infiltrometer and the leveled soil surface. Both infiltration experiments were carried out with pressure head $h_0 = -3.0$ cm. The instrument's cumulative infiltration measurements were compared to manual readings.

Another experiment was conducted in the mountainous Uhlířská experimental catchment on September 9th, 2012. Infiltration experiments were conducted on a leveled soil surface after the upper 30 cm of soil was removed. Experiments were conducted using tension $h_0 = -3.0$ cm.

Sets of undisturbed soil samples (137 cm^3) were taken from each location before the experiments. The initial and saturated volumetric water contents were determined gravimetrically for each undisturbed soil sample (Table 1).

Results of the infiltration experiment at the meadow site in the Kopaninský Stream catchment are shown in Fig. 6. Both infiltration rate and cumulative infiltration rate are well approximated by eq. (5) and (6) respectively (optimal parameter values $C_1 = 0.024$ cm $min^{-0.5}$ and $C_2 = 0.044$ cm min^{-1}). Figure 6 also demonstrate very good agreement between values obtained from automatic (empty symbols) and manual (filled symbols) readout of the water level during the infiltration experiment.

The quality of the measured data was assessed with regard to the possibility of loss of hydraulic contact between the soil surface and sintered steel disk or unwanted effects of the contact sand layer on infiltration. Differential linearization (Vandervaere et al., 1997) is shown in Fig. 7 for the dataset from meadow in Kopaninský Stream catchment. The data are apparently without significant deficiencies and are therefore suitable for determination of hydraulic conductivity.

The low *RMSE* values in Table 4 (less than 0.047 cm) indicate that the measured data are closely approximated by eq. (5). This implies that the major assumptions behind Philip's solution (e.g., homogeneity of flow domain) were not significantly violated. Unsaturated hydraulic conductivities K_{h0} were determined using modified Zhang method.

Values of K_{-3cm} at the two sites in the Kopaninský Stream catchment differ significantly. Unsaturated hydraulic conductivity of soil in the meadow is approximately two times higher than the soil in the tilled field which is in contradiction with studies by Schwartz et al. (2003) or Kelishadi et al. (2014), who observed higher unsaturated conductivity in the tilled field than in the meadow for pressure head below –3 cm. However, as is generally known, there is a significant influence of the seasonal variability of soil hydraulic properties associated with agricultural practices (Alletto and Coquet, 2009; Bodner et al., 2013; Castellini and Ventrella, 2012; Logsdon et al., 1993). Thus, lower unsaturated hydraulic conductivity in the field site is probably a consequence of macropore formation after postharvest stubble-breaking.

Hydraulic conductivities in the Uhlířská catchment are in a good agreement with values obtained previously using a manual tension infiltrometer (Soilmoisture Equipment Corp., Santa Barbara, CA; disk diameter of 20 cm), compare average value of 0.0029 cm min^{-1} and average value of 0.0035 cm min^{-1} computed from Table 4. The difference between K_{-3cm} and saturated hydraulic conductivity determined from ponded infiltration tests (Šanda, 1999) is more than four orders of magnitude which was expected for soil with strong preferential flow.

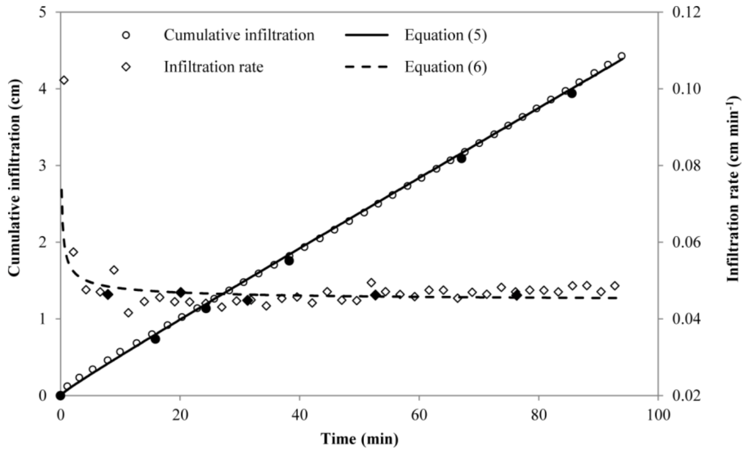

Fig. 6. Infiltration experiment results. Kopaninský Stream catchment (meadow site), August 2th, 2012.

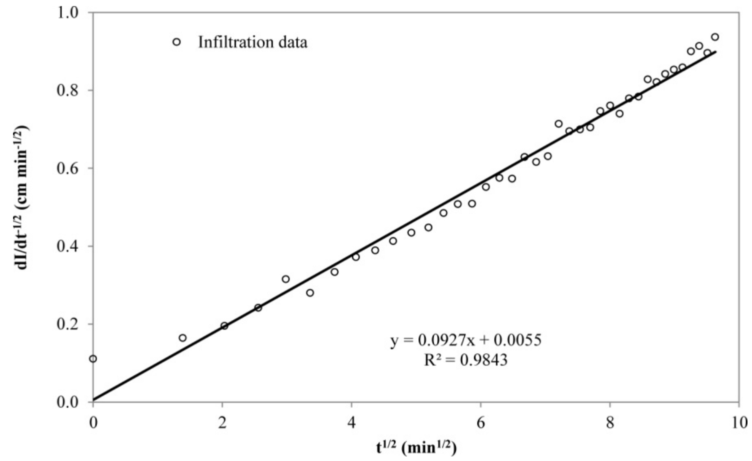

Fig. 7. Linearization of data set from the infiltration experiment carried out in the meadow location in the Kopaninský Stream catchment (August 2th, 2012). The differential linearization method was applied to the cumulative infiltration data set obtained from the instrument. Linearized data was fitted with solid line.

Table 4. Summary of the determined values of parameters C_1, C_2 including the root mean square error (*RMSE*) obtained from the best fit of measured cumulative infiltration data and values of near-saturated conductivity and sorptivity determined using modified Zhang method.

	C_1 (cm min$^{-1/2}$)	C_2 (cm min^{-1})	*RMSE* (cm)	A_1 (–)	A_2 (–)	K_{-3cm} (cm min^{-1})	S (cm min$^{-1/2}$)
Kopaninský Stream							
Meadow	0.024	0.044	0.026	1.403	4.726	0.0094	0.017
Tilled field	0.031	0.027	0.010	1.193	5.971	0.0046	0.026
Uhlířská							
Young forest	0.170	0.039	0.047	1.064	9.135	0.0042	0.160
	0.040	0.022	0.012	1.064	9.135	0.0024	0.037
	0.135	0.033	0.037	1.064	9.135	0.0037	0.127
	0.162	0.037	0.014	1.064	9.135	0.0040	0.152

CONCLUSIONS

The main objective of the paper was to test a newly developed automatic minidisk infiltrometer. The results show that the presented method of automation is fully functional. Comprehensive laboratory testing demonstrated the robustness of the AMI. The instrument/technique performed well in varying temperatures and during a bubbling test. The first tests of field application proved that AMI produces data sets of sufficient quality for determining near-saturated hydraulic conductivity.

Results of this study support the use of the operating principle of infiltration measurement on a wider scale. Running many automatic minidisk infiltrometers simultaneously will allow assessment of the spatial distribution of hydraulic conductivity.

Acknowledgements. This contribution has been supported by project Technology agency of Czech Republic No.: TA01021844 and project SGS No.: SGS14/131/OHK1/2T/11. We thank Pavel Tachecí for help with infiltration experiments and providing data of the retention curves, and David Zumr for his valuable input during development of infiltration module. We are also grateful to Philip Moravcik for his English-proofreading of the manuscript.

REFERENCES

Alletto, L., Coquet, Y., 2009. Temporal and spatial variability of soil bulk density and near-saturated hydraulic conductivity under two contrasted tillage management systems. Geoderma, 152, 1–2, 85-94.

Ankeny, M.D., Kaspar, T.C., Horton, R., 1988. Design for an automated tension infiltrometer. Soil Science Society of America Journal, 52, 3, 893–896.

Bodner, G., Scholl, P., Loiskandl, W., Kaul, H.P., 2013. Environmental and management influences on temporal variability of near saturated soil hydraulic properties. Geoderma, 204–205, 120–129.

Cameira, M.R., Fernando, R.M., Pereira, L.S., 2003. Soil macropore dynamics affected by tillage and irrigation for a silty loam alluvial soil in southern Portugal. Soil and Tillage Research, 70, 2, 131–140.

Castellini, M., Ventrella, D., 2012. Impact of conventional and minimum tillage on soil hydraulic conductivity in typical cropping system in Southern Italy. Soil and Tillage Research, 124, 47–56.

Dohnal, M., Dusek, J., Vogel, T., 2010. Improving hydraulic conductivity estimates from minidisk infiltrometer measurements for soils with wide pore-size distributions. Soil Science Society of America Journal, 74, 3, 804–811.

Doležal, F., Zumr, D., Vacek, J., Zavadil, J., Battilani, A., Plauborg, F.L., Hansen, S., Abrahamsen, P., Bízik, J., Takáč, J., Mazurczyk, W., Coutinho, J., Štekauerová, V., 2007. Dual permeability soil water dynamics and water uptake by roots in irrigated potato fields. Biologia, 62, 5, 552–556.

Gordon, D.C., Hallett, P.D., 2014. An automated microinfiltrometer to measure small-scale soil water infiltration properties. Journal of Hydrology and Hydromechanics, 62, 3, 252–256.

Holden, J., 2009. Topographic controls upon soil macropore flow. Earth Surface Processes and Landforms, 34, 3, 345–351.

Jara, V., Arellano, E., Baker, J., 2012. Using an automatic camera attached to minidisk infiltrometer to improve measurement in disturbed soils. In: Visions for a sustainable planet. ASA, CSSA, and SSSA International Annual Meetings, Oct. 21–24, 2012, Cincinnati, Ohio, USA.

Klute, A., 1986. Water retention: Laboratory methods. In: Klute, A. (Ed.): Methods of Soil Analysis, Part 1. Physical and Mineralogical Methods. American Society of Agronomy, Soil Science Society of America, Madison, Wisconsin, pp. 635–662.

Kelishadi, H., Mosaddeghi, M.R., Hajabbasi, M.A., Ayoubi, S., 2014. Near-saturated soil hydraulic properties as influenced by land use management systems in Koohrang region of central Zagros, Iran. Geoderma, 213, 426–434.

Lamparter, A., Deurer, M., Bachmann, J., Duijnisveld, W.H.M., 2006. Effect of subcritical hydrophobicity in a sandy soil on water infiltration and mobile water content. Journal of Plant Nutrition and Soil Science – Zeitschrift für Pflanzenernahrung und Bodenkunde, 169, 1, 38–46.

Li, X.Y., Gonzalez, A., Sole-Benet, A., 2005. Laboratory methods for the estimation of infiltration rate of soil crusts in the Tabernas Desert badlands. Catena, 60, 3, 255–266.

Logsdon, S.D., Jordahl, J.L., Karlen, D.L., 1993. Tillage and crop effects on ponded and tension infiltration rates. Soil and Tillage Research, 28, 2, 179–189.

Logsdon, S.D., Jaynes, D.B., 1996. Spatial variability of hydraulic conductivity in a cultivated field at different times. Soil Science Society of America Journal, 60, 3, 703–709.

Madsen, M.D., Chandler, D.G., 2007. Automation and use of mini disk infiltrometers. Soil Science Society of America Journal, 71, 5, 1469–1472.

Moret-Fernández, D., González, C., Lampurlanés, J., Vicente, J., 2012. An automated disc infiltrometer for infiltration rate measurements using a microflowmeter. Hydrological Processes, 26, 2, 240–245.

Moret, D., Lopez, M.V., Arrue, J.L., 2004. TDR application for automated water level measurement from Mariotte reservoirs in tension disc infiltrometers. Journal of Hydrology, 297, 1–4, 229–235.

Rodný, M., Rodný, P., Šurda, P., Matula, S., Miháliková, M., Chala, A. T., 2013. Automation of mini disk infiltrometer based on particle tracking principle. Acta Hydrologica Slovaca, 14, 2, 460–465.

Šanda, M., 1999. Runoff formation in the hillslope subsurface. Doctoral thesis. CTU in Prague, Prague. (In Czech.)

Schwartz, R.C., Evett, S.R., Unger, P.W., 2003. Soil hydraulic properties of cropland compared with reestablished and native grassland. Geoderma 116, 1–2, 47–60.

Schwarzel, K., Carrick, S., Wahren, A., Feger, K.H., Bodner, G., Buchan, G., 2011. Soil hydraulic properties of recently tilled soil under cropping rotation compared with two-year Pasture. Vadose Zone Journal, 10, 1, 354–366.

Tachecí, P., Žlábek P., Kvítek T., Peterková J., 2013. Analysis of rainfall-runoff events on four subcatchments of Kopaninsky tok (Czech Republic). Bodenkultur, 64, 3–4, 105–111.

van Genuchten, M.Th., 1980. A closed form equation for predicting the hydraulic conductivity of unsatured soils. Soil Science Society of America Jurnal, 44, 892–898.

Vandervaere, J.P., Peugeot, C., Vauclin, M., Jaramillo, R.A., Lebel, T., 1997. Estimating hydraulic conductivity of crusted soils using disc infiltrometers and minitensiometers. Journal of Hydrology, 189, 1–4, 203–223.

Vandervaere, J.P., Vauclin, M., Elrick, D.E., 2000. Transient flow from tension infiltrometers: I. The two-parameter equation. Soil Science Society of America Journal, 64, 4, 1263–1272.

Vervoort, R.W., Radcliffe, D.E., West, L.T., 1999. Soil structure development and preferential solute flow. Water Resources Research, 35, 4, 913–928.

Vervoort, R.W., Cattle, S.R., Minasny, B., 2003. The hydrology of Vertosols used for cotton production: I. Hydraulic, structural and fundamental soil properties. Australian Journal of Soil Research, 41, 7, 1255–1272.

Warrick, A.W., Broadbridge, P., 1992. Sorptivity and macroscopic capillary length relationships. Water Resources Research, 28, 427–431.

White, I., Sully, M.J., Perroux, K.M., 1992. Measurement of surface-soil hydraulic-properties - disk permeameters, tension infiltrometers, and other techniques. Advances in Measurement of Soil Physical Properties: Bringing Theory into Practice, 30, 69–103.

Zhang, R.D., 1997. Determination of soil sorptivity and hydraulic conductivity from the disk infiltrometer. Soil Science Society of America Journal, 61, 4, 1024–1030.

Received 5 December 2014
Accepted 18 February 2015

Note: Colour version of Figures can be found in the web version of this article.